PERGAMON

International Journal of Solids and Structures 37 (2000) 6221–6237

INTERNATIONAL JOURNAL OF SOLIDS and STRUCTURES

www.elsevier.com/locate/ijsolstr

Asymptotic bounds on overall moduli of cracked bodies

J. Wang[a], J. Fang[a], B.L. Karihaloo[b,*]

[a]*Department of Mechanics and Engineering Science, Peking University, Beijing 100871, People's Republic of China*
[b]*Cardiff School of Engineering, University of Wales Cardiff, Queen's Buildings, P.O. Box 686, Cardiff CF2 3TB, UK*

Received 9 November 1998; in revised form 7 September 1999

Abstract

The interactions among multiple parallel microcracks in an elastic body are examined asymptotically in an explicit and quantitative manner in order to reveal fully their so-called shielding and magnification effects on the overall moduli of the body. Based upon this asymptotic analysis, analytical upper and lower bounds are proposed for the overall moduli of bodies containing randomly distributed multiple parallel unbridged/bridged microcracks. The bounds are used to assess the accuracy of the approximate methods —the dilute distribution approximation, the differential scheme and the self-consistent model — that are commonly used to determine the overall moduli of bodies containing multiple microcracks.

Keywords: Asymptotic bounds; Cracked bodies; Overall moduli; Crack shielding; Crack amplification; Multiple cracks; Crack interaction

1. Introduction

The first and foremost sign of tensile damage in fibre-reinforced brittle matrices, such as ceramics and cements, is the appearance of multiple parallel microcracks. They cause the stress–strain curve to deviate from linearity, i.e. give the composite a strain-hardening response. Bridging of the multiple microcracks by short fibres is an important mechanism for increasing the toughness of these composites and for preventing a sudden loss of their overall stiffness when the microcracks coalesce and localise into large bands. The prediction of the effective elastic and fracture properties of a medium containing multiple cracks has, therefore, received considerable attention. Among the studies are the solutions based upon the non-interacting approximation, when the interaction among the cracks is neglected. Under this

* Corresponding author. Tel.: +44-1222-874-934; fax: +44-1222-874-597.
E-mail address: karihaloob@cardiff.ac.uk (B.L. Karihaloo).

0020-7683/00/$ - see front matter
PII: S0020-7683(99)00258-9

assumption, the effective elastic properties can be expressed in explicit forms. According to Kachanov (1992), the non-interacting solution is the only non-controversial approximation to the problem.

The interactions among multiple cracks complicate the prediction of the overall moduli. The schemes based upon indirect considerations of crack interactions, such as the self-consistent method and the differential scheme may considerably underestimate the overall moduli, as has been pointed out by Kachanov (1992) and Ju and Chen (1994).

When attempting to predict the overall moduli of bodies containing multiple microcracks, one is faced with many major difficulties. Firstly, one is faced with the question as to whether the interactions increase or decrease the overall moduli compared with the results obtained neglecting the interactions. Secondly, although various methods have been proposed to predict the overall moduli of bodies containing multiple microcracks, the accuracy of these methods cannot be judged due to a lack of proper bounds. Thirdly, as pointed out by Kachanov (1992), no non-trivial upper or lower bounds can be found that are valid for any particular sample of a given crack statistics. It should be noted that Wu and Chudnovsky (1990) proposed upper and lower bounds for the overall Young modulus of bodies containing multiple parallel cracks at very high crack density. Their bounds were obtained based upon a simple beam model and the omission of interactions among the crack rows. Kachanov (1992) also pointed out some questionable published results on the bounds of overall moduli of cracked bodies.

In the present paper, we attempt to obtain the upper and lower bounds on the overall moduli of elastic bodies containing multiple parallel random microcracks in the two-dimensional approximation. For this, we examine the so-called "shielding" and "magnification" interaction effects among the multiple cracks (Kachanov, 1992). It is found that the crack interactions under unidirectional tension and in-plane shear have opposite effects on the overall moduli. Through this examination of interaction effects and an asymptotic analysis (Wang et al., 1999), the upper and lower bounds on the Young and in-plane shear moduli are obtained in concise explicit forms for both unbridged and bridged cracks as functions of the conventional crack density parameter. For unbridged cracks, the bounds are compared with the dilute distribution solution, the differential scheme and the self-consistent model for a quantitative assessment of these approximate methods as they are applied to the evaluation of the overall moduli of bodies containing multiple parallel microcracks. For bridged cracks, the results reveal the competing effects of crack interactions and the bridging force on the overall moduli of cracked bodies. Although only the two-dimensional problem is considered in this paper, the principle is believed to be equally applicable to the three-dimensional case.

2. General formulae and crack interactions

2.1. General formulae

The overall (average) strain and stress of a cracked body are related via (e.g. Kachanov, 1992)

$$\varepsilon_{ij} = C^0_{ijkl}\sigma_{kl} + \frac{1}{2V}\sum^{N}\int_{S_N}\left([u_i]n_j + [u_j]n_i\right)\mathrm{d}S_N \tag{1}$$

where σ_{kl} and ε_{ij} are the average stress and strain components, respectively. u_i and n_i are the total crack opening/sliding displacement (COD/CSD) and the component of the unit vector normal to the crack faces. C^0_{ijkl} is the compliance tensor of the uncracked material. N and S_N denote the number of a crack and the area of its faces. For parallel flat cracks when n_i is a constant, Eq. (1) can be rewritten as

$$\varepsilon_{ij} = C^{0}_{ijkl}\sigma_{kl} + \frac{1}{2V}\sum^{N}\left([\bar{u}_i]n_j + [\bar{u}_j]n_i\right)S_N \tag{2}$$

where $[\bar{u}_i]$ is the average COD/CSD for a single crack over its faces.

The average COD/CSD $[\bar{u}_i]$ can be expressed through a second-order tensor B_{ij}

$$[\bar{u}_i] = B_{ij}t_j \tag{3}$$

where t_j is a uniform traction applied on the crack faces. Eq. (3) is only valid when the opening/sliding traction on the crack faces is a constant. For an isotropic material, the second-order tensor B_{ij} can be easily obtained. We now return to the determination of the traction t_j.

For an isolated frictionless crack in an infinite body under a far-field stress σ^0_{ij}, $[\bar{u}_i]$ can be expressed as follows

$$[\bar{u}_i] = B_{il}\sigma^0_{lk}n_k \tag{4}$$

For a body containing multiple cracks, the effect of crack interactions and of any bridging tractions must be taken into account in the calculation of the COD/CSD. Using the pseudo-traction formalism, the average COD/CSD is solely determined by the pseudo-traction, i.e.,

$$[\bar{u}_i] = B_{il}\sigma^{\mathrm{p}}_{lk}n_k \tag{5}$$

where we assume that the pseudo-traction σ^{p}_{lk} is a constant on the crack faces and is given by

$$\sigma^{\mathrm{p}}_{ij} = T_{ijkl}\sigma^0_{kl} \tag{6}$$

T_{ijkl} is a fourth-order transformation tensor relating the crack opening/sliding stress to the applied stress. It is equivalent to the interaction matrix Λ_{ij} in the work of Kachanov (1987).

Thus, we can express the average COD/CSD $[\bar{u}_i]$ in the following form

$$[\bar{u}_i] = B_{il}T_{lkmn}\sigma^0_{mn}n_k \tag{7}$$

For a body containing multiple parallel microcracks under prescribed stress boundary conditions, the average stress σ_{ij} in Eq. (1) is equal to σ^0_{ij} of Eq. (7) (Horii and Nemat-Nasser, 1985; Karihaloo et al., 1996). Substitution of Eq. (7) into Eq. (2) yields

$$\varepsilon_{ij} = C^{0}_{ijkl}\sigma^0_{kl} + \frac{1}{2V}\sum^{N}\left(B_{il}T_{lkmn}\sigma^0_{mn}n_kn_j + B_{jl}T_{lkmn}\sigma^0_{mn}n_kn_i\right)S_N \tag{8}$$

which can be rewritten as

$$\varepsilon_{ij} = \left(C^{0}_{ijkl} + \Delta C_{ijkl}\right)\sigma^0_{kl} \tag{9}$$

where

$$\Delta C_{ijkl} = \frac{1}{2V}\sum^{N}\left(B_{ip}T_{pqmn}I_{mnkl}n_qn_j + B_{jp}T_{pqmn}I_{mnlk}n_qn_i\right)S_N \tag{10}$$

I_{mnkl} is the symmetric fourth-order unit tensor.

Within the formalism of pseudo-tractions, the COD/CSD $[u_i]$ is calculated by applying a pseudo-traction on the faces of a single crack or a row of collinear cracks in an infinite medium. Thus, the

tensor B_{ij} in Eq. (3) is determined only by the elastic properties of the medium under consideration. On the other hand, the transformation tensor T_{ijkl} is related to the interaction among the cracks. Therefore, if the configuration of the parallel microcracks, but not their density, is such that the magnitude of the transformation tensor T_{ijkl}, or at least the magnitude of some of its major components, is maximised, then the interaction among the cracks will create the maximum increase in ΔC_{ijkl} and thus the maximum decrease in the overall moduli of the cracked body. On the other hand, if the configuration is such that T_{ijkl} is minimised, then the minimum decrease in the overall moduli can be expected. These two extreme cases would correspond to the strongest "magnification" and the strongest "shielding" interaction effects in the terminology introduced by Kachanov (1992). The effect of a natural configuration of multiple cracks on the overall moduli of a cracked body should be between these two extreme effects. In the sequel, we shall seek to estimate these extreme interaction effects among the multiple microcracks.

2.2. Crack interactions

For two-dimensional parallel cracks, we need to evaluate collinear and stacked interactions (Wang et al., 1999). A previous study (Wang et al., 1999) of a doubly periodic array of cracks showed that the stacked interaction has a significant influence on the magnitude of the pseudo-traction on the crack faces and thus on the overall moduli of the cracked body. The collinear effect has been previously investigated by Kachanov (1987). In this paper, we will use the model shown in Fig. 1 to investigate the interactions among multiple parallel microcracks in an isotropic medium.

Let us suppose that the body contains a row of collinear cracks represented by the solid lines and that a new group of cracks will emerge in the area adjacent to these represented by the broken lines. The location of one of the newly-emerged cracks is represented by the line segment AB. We assume further that the newly-emerged crack is of the same size as the existing cracks. Let us now examine the interaction among the existing collinear cracks and the newly-emerged cracks. For this, we neglect the mutual collinear interactions among the new cracks but concentrate on the interaction among the existing collinear cracks and a single representative new crack, namely, crack AB.

Let the body be subjected to a far-field stress σ^0_{ij}, so that the opening/sliding stress $p^{AB}_{ij}(x, H)$ at the potential location of crack AB, which has to be annulled, can be expressed as

$$p^{AB}_{ij}(x, H) = T'_{ijkl}(x, H)\sigma^0_{kl} \tag{11}$$

where the components of $T'_{ijkl}(x, H)$ represent the stress components $\sigma_{ij}(x, H)$ induced at the point (x, H) when the body containing the collinear cracks is subjected to a unit far-field stress. Here, for simplicity of analysis, we shall ignore the multiple reflection effects of the crack AB and the collinear cracks. Taking the average of $p^{AB}_{ij}(x, H)$ over the crack length $2a$, we get

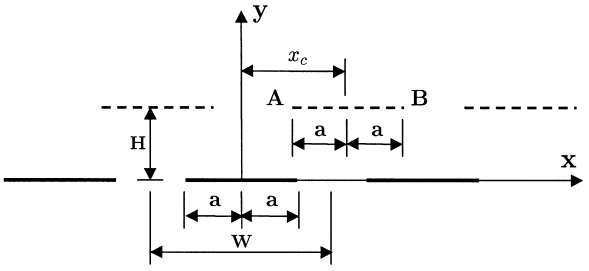

Fig. 1. Interacting cracks. Solid lines represent existing cracks, and dashed lines represent emerging cracks.

$$\left\langle p_{ij}^{\mathrm{AB}}(x_{\mathrm{c}}, H)\right\rangle = T_{ijkl}(x_{\mathrm{c}}, H)\sigma_{kl}^{0} \tag{12}$$

where x_{c} is the x-coordinate of the centre of the crack AB, and

$$T_{ijkl}(x_{\mathrm{c}}, H) = \frac{1}{2a}\int_{x_{\mathrm{c}}-a}^{x_{\mathrm{c}}+a} T'_{ijkl}(x, H)\,\mathrm{d}x \tag{13}$$

Let us now examine the variations of $T_{ijkl}(x_{\mathrm{c}}, H)$ in order to characterise the crack interactions. Firstly, let the body be subjected to $\sigma_{22}^{0}\neq 0$ or $\sigma_{12}^{0}\neq 0$. Under these loading conditions, we only study the non-trivial components $T_{1222}(x_{\mathrm{c}}, H)$, $T_{2222}(x_{\mathrm{c}}, H)$, $T_{2212}(x_{\mathrm{c}}, H)$ and $T_{1212}(x_{\mathrm{c}}, H)$. As $T'_{ijkl}(x, H)$ can be obtained in closed forms from the formulae in the handbook by Tada et al. (1973), $T'_{ijkl}(x_{\mathrm{c}}, H)$ can be easily calculated. The variations of these components with the normalised crack spacings W/a and H/a are shown in Figs. 2 and 3 for $W/a = 3.0$ and $W/a = 2.2$, respectively.

It is seen from Figs. 2 and 3 that coupling components T_{1222} and T_{2212} are much smaller than the principal components T_{1212} and T_{2222}. Thus, we shall not discuss the coupling terms, but concentrate

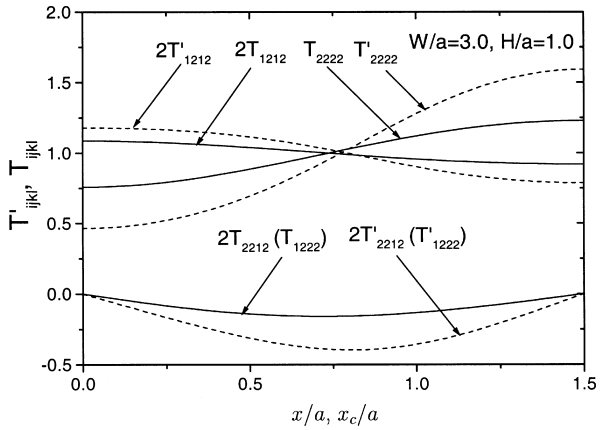

(a)

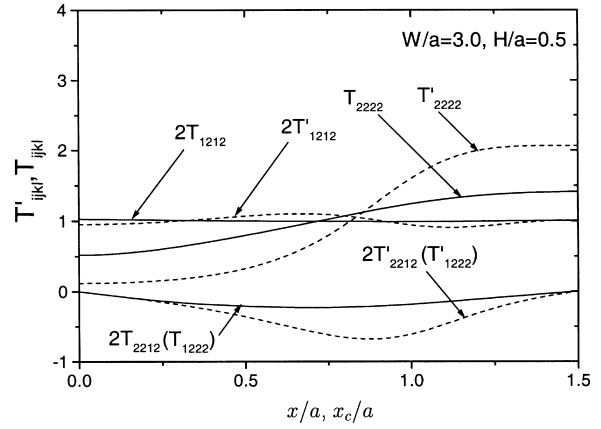

(b)

Fig. 2. Variations of $T'_{ijkl}(x/a, H/a)$ and $T_{ijkl}(x_{\mathrm{c}}/a, H/a)$ for interacting cracks for $W/a = 3.0$.

only on the principal terms. T'_{2222} and T_{2222} attain their respective maxima at $x = W/2$ and $x_c = W/2$. Due to symmetry of the problem, $T'_{1212}(x, H)$ and $T'_{2222}(x, H)$ must attain local extrema at $x = W/2$. When W/a is large, these extrema are likely to be their local minima because the stress concentrations shift to the areas around the crack tips. However, for the two cases considered in Figs. 2 and 3, the extrema of T'_{2222} turn out to be its maxima. The maximum of T'_{1212} is at $x = 0$, except for $W/a = 2.2$ and $H/a = 0.5$ when it appears to be shifted. Even then, the maximum value of T'_{1212} is only marginally larger than its value at $x = 0$. Nevertheless, for $W/a = 2.2$ and $H/a = 0.5$, the maximum of T_{2222} is still at $x = W/2$. From the above observations we can conclude that under unidirectional tension, the crack AB will experience the strongest shielding effect when it is situated immediately above one of the existing collinear cracks and that it will experience the strongest magnification effect when it straddles two existing collinear cracks below it. The interaction effects under in-plane shear loading are the opposite. We note that when H/a is very small, the transformation tensor may exhibit different variations. However, it is seen that as H/a is very small both T'_{1212} and T'_{2222} tend to zero in the area close to the crack faces. Thus, it is unlikely that new cracks will appear in these areas of significant

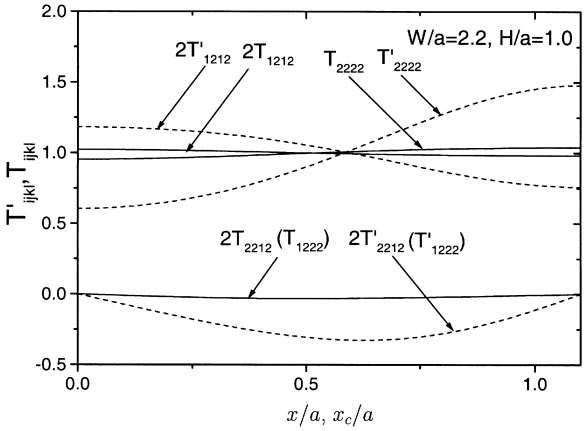

(a)

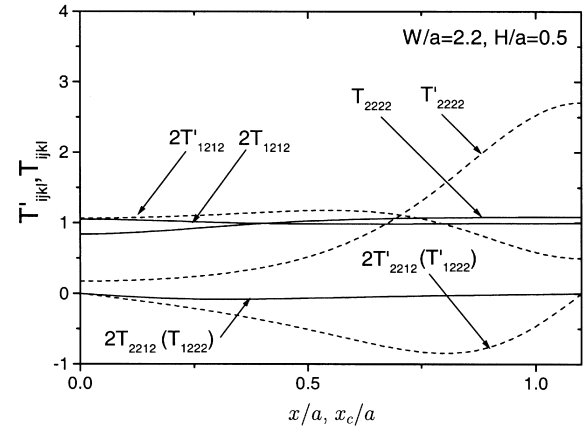

(b)

Fig. 3. Variations of $T'_{ijkl}(x/a, H/a)$ and $T_{ijkl}(x_c/a, H/a)$ for interacting cracks for $W/a = 2.2$ in Fig. 1.

stress relaxation. On the other hand, new cracks may appear in-between two existing collinear cracks. This simply reduces W/a, which does not alter the above conclusions.

3. Periodic arrays of cracks and asymptotic analysis

It follows from the above observations that, if multiple cracks in a body are so arranged that every crack is subjected to the strongest shielding effect from the remaining cracks, the crack interactions will cause the least reduction in the overall moduli of the body. Conversely, if the cracks are so arranged that every crack is subjected to the strongest magnification effect from the remaining cracks, the crack interactions will cause the most reduction in the overall moduli of the body. The real situation will lie somewhere between these two extremes. Based upon the study of the crack interactions in Section 2.2, the two extreme crack arrangements are found to be the periodic rectangular array of cracks and the diamond-shaped array of cracks, shown in Fig. 4. These two types of arrays of unbridged cracks have been previously studied by Karihaloo (1978) in the context of elastoplastic fracture mechanics.

From the analysis of the crack interactions in Section 2.2 under unidirectional tension perpendicular to the cracks, the cracks in the doubly periodic rectangular array will experience the strongest shielding effect, and those in the diamond-shaped array will experience the strongest magnification effect. On the other hand, under in-plane shear, the cracks in the former will experience the strongest magnification effect, and those in the latter will experience the strongest shielding effect.

In order to calculate the overall moduli, or ΔC_{ijkl} in Eq. (10), corresponding to the two arrays of cracks, we need to calculate the transformation tensor T_{ijkl}. As can be seen from Eq. (10), for the prediction of the major compliance components ΔC_{2222} and ΔC_{1212}, we need only to calculate T_{1212} and T_{22222} for the two arrays. For this, we use the procedures described in the work of Karihaloo et al. (1996), and recently of Wang et al. (1999). Karihaloo et al. (1996) solved the doubly periodic rectangular array of unbridged/bridged cracks using a superposition procedure and the pseudo-traction technique (Horii and Nemat-Nasser, 1985; Hu et al., 1994). Wang et al. (1999) obtained an explicit expression for the overall Young modulus for a body containing a doubly periodic rectangular array of unbridged/bridged cracks using an asymptotic analysis. Here, we solve the two arrays of cracks in Fig. 4 following the procedures in the two papers by Karihaloo et al. (1996) and Wang et al. (1999). We consider first arrays of unbridged cracks and then of bridged cracks.

Following the procedure of Karihaloo et al. (1996), the traction consistency condition on each crack in either of the two arrays shown in Fig. 4 can be written as

$$\sigma^{\mathrm{p}}_{ij}(x) - 2\sum_{j=1}^{+\infty}\int_0^a K_{ijkl}(x, x^{\,j})\sigma^{\mathrm{p}}_{kl}(x^{\,j})\,\mathrm{d}x^{\,j} + p_{ij}(x) = \sigma^0_{ij} \quad x \in [0, a) \tag{14}$$

where $\sigma^{\mathrm{p}}_{ij}(x)$ is the pseudo-traction on the crack faces, $p_{ij}(x)$ is the bridging stress, and σ^0_{ij} is the applied stress. The meanings of x and $x^{\,j}$ are indicated in the papers by Karihaloo et al. (1996) and Karihaloo

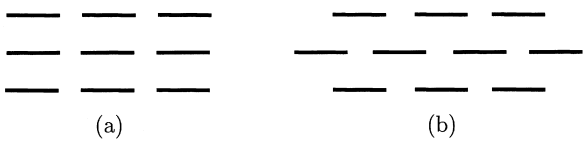

Fig. 4. Doubly periodic rectangular array of cracks (a) and diamond-shaped array of cracks (b) that exhibit the strongest shielding and magnification effects, respectively.

and Wang (1997). Following Horii and Nemat-Nasser (1985) and Karihaloo et al. (1996), the stress σ_{ij}^0 is regarded as a homogeneous stress in the same body if all the cracks were absent. Due to symmetry, the pseudo-traction is the same on all cracks in each array. The second term in the left-hand side of Eq. (14) represents the interaction among all the cracks. K_{ijkl} are equivalent in form and effect to T'_{ijkl}. Thus, we can also neglect the coupling terms and consider only the principal terms K_{2222} and K_{1212}. The expression for $K_{2222}(x, x^j)$ was given by Karihaloo and Wang (1997)

$$
\begin{aligned}
K_{2222}(x, x^j) = \frac{2}{W}\mathrm{Re}\left\{ \frac{\cos(\pi x^j/W)\sqrt{(\sin(\pi a/W))^2-(\sin(\pi x^j/W))^2}}{\left[(\sin(\pi z/W))^2-(\sin(\pi x^j/W))^2\right]\sqrt{1-(\sin(\pi a/W)/\sin(\pi z/W))^2}} \right\} \\
-\frac{2y}{W}\mathrm{Im}\left\{ \frac{\cos(\pi x^j/W)\sqrt{(\sin(\pi a/W))^2-(\sin(\pi x^j/W))^2}}{\left[(\sin(\pi z/W))^2-(\sin(\pi x^j/W))^2\right]^2\left[1-(\sin(\pi a/W)/\sin(\pi z/W))^2\right]} \right. \\
\left. \times \left[2\frac{\pi}{W}\sin\frac{\pi z}{W}\cos\frac{\pi z}{W}\sqrt{1-(\sin(\pi a/W)/\sin(\pi z/W))^2} \right.\right. \\
\left.\left. +\frac{\pi}{W}\frac{(\sin(\pi a/W))^2\cos(\pi z/W)\left[(\sin(\pi z/W))^2-(\sin(\pi x^j/W))^2\right]}{(\sin(\pi z/W))^3\sqrt{1-(\sin(\pi a/W)/\sin(\pi z/W))^2}} \right] \right\}
\end{aligned}
\tag{15}
$$

where $z = x + iy = x + i(jH)$ ($i = \sqrt{-1}$, $j = 1, 2, \ldots, +\infty$). $K_{1212}(x, x^j)$ is also easily obtained using the formulae in the handbook by Tada et al. (1973)

$$
\begin{aligned}
K_{1212}(x, x^j) = \frac{1}{W}\mathrm{Re}\left\{ \frac{\cos(\pi x^j/W)\sqrt{(\sin(\pi a/W))^2-(\sin(\pi x^j/W))^2}}{\left[(\sin(\pi z/W))^2-(\sin(\pi x^j/W))^2\right]\sqrt{1-(\sin(\pi a/W)/\sin(\pi z/W))^2}} \right\} \\
-\frac{y}{W}\mathrm{Im}\left\{ \frac{\cos(\pi x^j/W)\sqrt{(\sin(\pi a/W))^2-(\sin(\pi x^j/W))^2}}{\left[(\sin(\pi z/W))^2-(\sin(\pi x^j/W))^2\right]^2\left[1-(\sin(\pi a/W)/\sin(\pi z/W))^2\right]} \right. \\
\left. \times \left[2\frac{\pi}{W}\sin\frac{\pi z}{W}\cos\frac{\pi z}{W}\sqrt{1-(\sin(\pi a/W)/\sin(\pi z/W))^2} \right.\right. \\
\left.\left. +\frac{\pi}{W}\frac{(\sin(\pi a/W))^2\cos(\pi z/W)\left[(\sin(\pi z/W))^2-(\sin(\pi x^j/W))^2\right]}{(\sin(\pi z/W))^3\sqrt{1-(\sin(\pi a/W)/\sin(\pi z/W))^2}} \right] \right\}
\end{aligned}
\tag{16}
$$

For a given loading condition, the integral equation (14) can be easily and accurately solved using Gauss–Legendre quadrature. After solving $\sigma_{ij}^{\mathrm{p}}(x)$ from Eq. (14), the stress intensity factor and the COD/

CSD can be easily calculated numerically, as can the overall moduli of the cracked body (Karihaloo et al., 1996).

As in the work of Wang et al. (1999), we aim to obtain an approximate closed-form solution of the integral equation (14) for the two arrays in Fig. 4. To this end, we assume that the cracks are so distributed that the higher-order terms (in comparison with terms of order 1) containing $e^{-1(H/W)\pi}$ $(1 \geq 4j)$, $e^{-n(H/W)\pi}\sin^m(\pi a/W)$ and $e^{-n(H/W)\pi}\sin^m(\pi x/W)$ $(n \geq 2j$ and $m \geq 2)$ either singly or in any combination in K_{2222} and K_{1212} in Eqs. (15) and (16) can be neglected. Throughout this paper, the term "asymptotic" is used to emphasise this assumption, and the phrase "asymptotic analysis" is used for the approximate analytical procedure and results obtained on the basis of this assumption. The asymptotic expressions for $K_{2222}(x, x^j)$ and $K_{1212}(x, x^j)$ for the two arrays of Fig. 4 are

$$\begin{Bmatrix} K^{\mathrm{r}}_{2222}(x, x^j) \\ K^{\mathrm{d}}_{2222}(x, x^j) \\ K^{\mathrm{r}}_{1212}(x, x^j) \\ K^{\mathrm{d}}_{1212}(x, x^j) \end{Bmatrix} = \begin{Bmatrix} -2\left[1 + 2j\dfrac{H}{W}\pi\right] \\ 2\left[1 + 2j\dfrac{H}{W}\pi\right] \\ -\left[1 - 2j\dfrac{H}{W}\pi\right] \\ \left[1 - 2j\dfrac{H}{W}\pi\right] \end{Bmatrix} \frac{4}{W} e^{-2j(H/W)\pi} \cos\frac{\pi x^j}{W} \sqrt{\sin^2\frac{\pi a}{W} - \sin^2\frac{\pi x^j}{W}} \tag{17}$$

where the superscripts r and d refer to the rectangular and diamond-shaped array, respectively. Substituting Eq. (17) into Eq. (14) gives

$$\sigma^{\mathrm{p}}_{22}(x) - 2\sum_{j=1}^{+\infty} \int_0^a \begin{Bmatrix} K^{\mathrm{r}}_{2222}(x, x^j) \\ K^{\mathrm{d}}_{2222}(x, x^j) \end{Bmatrix} \sigma^{\mathrm{p}}_{22}(x^j)\, \mathrm{d}x^j + p_{22}(x) = \sigma^0_{22} \tag{18}$$

$$\sigma^{\mathrm{p}}_{12}(x) - 4\sum_{j=1}^{+\infty} \int_0^a \begin{Bmatrix} K^{\mathrm{r}}_{1212}(x, x^j) \\ K^{\mathrm{d}}_{1212}(x, x^j) \end{Bmatrix} \sigma^{\mathrm{p}}_{12}(x^j)\, \mathrm{d}x^j + p_{12}(x) = \sigma^0_{12} \tag{19}$$

For unbridged cracks, i.e. $p_{22}(x) = 0$ and $p_{12}(x) = 0$, Eqs. (18) and (19) reduce to

$$\sigma^{\mathrm{p}}_{22}(x) - 2\sum_{j=1}^{+\infty} \int_0^a \begin{Bmatrix} K^{\mathrm{r}}_{2222}(x, x^j) \\ K^{\mathrm{d}}_{2222}(x, x^j) \end{Bmatrix} \sigma^{\mathrm{p}}_{22}(x^j)\, \mathrm{d}x^j = \sigma^0_{22} \tag{20}$$

$$\sigma^{\mathrm{p}}_{12}(x) - 4\sum_{j=1}^{+\infty} \int_0^a \begin{Bmatrix} K^{\mathrm{r}}_{1212}(x, x^j) \\ K^{\mathrm{d}}_{1212}(x, x^j) \end{Bmatrix} \sigma^{\mathrm{p}}_{12}(x^j)\, \mathrm{d}x^j = \sigma^0_{12} \tag{21}$$

As the kernels $K^{\mathrm{r}}_{2222}(x, x^j)$, $K^{\mathrm{d}}_{2222}(x, x^j)$, $K^{\mathrm{r}}_{1212}(x, x^j)$ and $K^{\mathrm{d}}_{1212}(x, x^j)$ in the Eqs. (20) and (21) do not contain the variable x, the pseudo-tractions $\sigma^{\mathrm{p}}_{22}(x)$ and $\sigma^{\mathrm{p}}_{12}(x)$ which satisfy these equations must be independent of x, that is, they must be constant on the crack faces. Thus, $\sigma^{\mathrm{p}}_{22}(x)$ and $\sigma^{\mathrm{p}}_{12}(x)$ are given by (after carrying out the indicated integrations and summations)

$$\begin{Bmatrix} \sigma_{22}^{pr} \\ \sigma_{22}^{pd} \end{Bmatrix} = \begin{Bmatrix} \alpha^{r} \\ \alpha^{d} \end{Bmatrix} \sigma_{22}^{0} \tag{22}$$

$$\begin{Bmatrix} \sigma_{12}^{pr} \\ \sigma_{12}^{pd} \end{Bmatrix} = \begin{Bmatrix} \beta^{r} \\ \beta^{d} \end{Bmatrix} \sigma_{12}^{0} \tag{23}$$

where

$$\alpha^{r} = \frac{1}{1 + 4\sin^2(\pi a/W)\, e^{-2(H/W)\pi}\left[1 + 2(H/W)\pi\right]} \tag{24}$$

$$\alpha^{d} = \frac{1}{1 - 4\sin^2(\pi a/W)\, e^{-2(H/W)\pi}\left[1 + 2(H/W)\pi\right]} \tag{25}$$

$$\beta^{r} = \frac{1}{1 + 4\sin^2(\pi a/W)\, e^{-2(H/W)\pi}\left[1 - 2(H/W)\pi\right]} \tag{26}$$

$$\beta^{d} = \frac{1}{1 - 4\sin^2(\pi a/W)\, e^{-2(H/W)\pi}\left[1 - 2(H/W)\pi\right]} \tag{27}$$

On the other hand, when the cracks are bridged, various bridging laws can be chosen in the numerical solution of Eq. (14). In the present study, we choose the simple linear bridging laws as follows

$$p_{22}(x) = k_{22}[u_2](x), \qquad p_{12}(x) = k_{12}[u_1](x) \tag{28}$$

where k_{22} and k_{12} are the bridging stiffnesses, and $[u_2](x)$ and $[u_1](x)$ are the COD and CSD. Such linear bridging laws occur, for example, when the material is reinforced with short fibres (Nemat-Nasser and Hori, 1987; Karihaloo et al., 1996).

Following the solution for the unbridged case, we assume constant pseudo-tractions $\sigma_{22}^{p}(x) = \sigma_{22}^{p}$ and $\sigma_{12}^{p}(x) = \sigma_{12}^{p}$ over the crack faces. Substituting the constant pseudo-tractions into Eqs. (18) and (19) reduces the left-hand sides of these equations to

$$\begin{Bmatrix} \dfrac{1}{\alpha^{r}} \\ \dfrac{1}{\alpha^{d}} \end{Bmatrix} \sigma_{22}^{p} + k_{22}[u_2](x) \tag{29}$$

$$\begin{Bmatrix} \dfrac{1}{\beta^{r}} \\ \dfrac{1}{\beta^{d}} \end{Bmatrix} \sigma_{12}^{p} + k_{12}[u_1](x) \tag{30}$$

It is evident that the traction consistency conditions (18) and (19) cannot be satisfied, because the expressions (29) and (30) are functions of x, whereas the right-hand sides of Eqs. (18) and (19) are constants, namely, σ_{22}^{0} and σ_{12}^{0}. For this reason, we approximate these traction consistency conditions in

an average sense as follows

$$\frac{1}{2a}\int_{-a}^{+a}\left[\left\{\begin{array}{c}\dfrac{1}{\alpha^{\mathrm{r}}}\\ \dfrac{1}{\alpha^{\mathrm{d}}}\end{array}\right\}\sigma_{22}^{\mathrm{p}}+k_{22}[u_2](x)\right]\mathrm{d}x=\sigma_{22}^{0} \tag{31}$$

$$\frac{1}{2a}\int_{-a}^{+a}\left[\left\{\begin{array}{c}\dfrac{1}{\beta^{\mathrm{r}}}\\ \dfrac{1}{\beta^{\mathrm{d}}}\end{array}\right\}\sigma_{12}^{\mathrm{p}}+k_{12}[u_1](x)\right]\mathrm{d}x=\sigma_{12}^{0} \tag{32}$$

The integrals $\int_{-a}^{+a}[u_2](x)\,\mathrm{d}x$ and $\int_{-a}^{+a}[u_1](x)\,\mathrm{d}x$ for a single crack in a periodic collinear crack array subjected to constant surface tractions can be found in the work by Deng and Nemat-Nasser (1992), whence Eqs. (31) and (32) yield

$$\left\{\begin{array}{c}\sigma_{22}^{\mathrm{pr}}\\ \sigma_{22}^{\mathrm{pd}}\end{array}\right\}=\left\{\begin{array}{c}\zeta^{\mathrm{r}}\\ \zeta^{\mathrm{d}}\end{array}\right\}\sigma_{22}^{0} \tag{33}$$

where

$$\left\{\begin{array}{c}\sigma_{12}^{\mathrm{pr}}\\ \sigma_{12}^{\mathrm{pd}}\end{array}\right\}=\left\{\begin{array}{c}\eta^{\mathrm{r}}\\ \eta^{\mathrm{d}}\end{array}\right\}\sigma_{12}^{0} \tag{34}$$

$$\zeta^{\mathrm{r}}=\left\{1-4\sin^2\frac{\pi a}{W}\mathrm{e}^{-2(H/W)\pi}\left[1+2\frac{H}{W}\pi\right]-\frac{2k_{22}W^2}{\pi aE'}\ln\left(\cos\frac{\pi a}{W}\right)\right\}^{-1} \tag{35}$$

$$\zeta^{\mathrm{d}}=\left\{1-4\sin^2\frac{\pi a}{W}\,\mathrm{e}^{-2(H/W)\pi}\left[1+2\frac{H}{W}\pi\right]-\frac{2k_{22}W^2}{\pi aE'}\ln\left(\cos\frac{\pi a}{W}\right)\right\}^{-1} \tag{36}$$

$$\eta^{\mathrm{r}}=\left\{1+4\sin^2\frac{\pi a}{W}\mathrm{e}^{-2(H/W)\pi}\left[1-2\frac{H}{W}\pi\right]-\frac{2k_{12}W^2}{\pi aE'}\ln\left(\cos\frac{\pi a}{W}\right)\right\}^{-1} \tag{37}$$

$$\eta^{\mathrm{d}}=\left\{1-4\sin^2\frac{\pi a}{W}\mathrm{e}^{-2(H/W)\pi}\left[1-2\frac{H}{W}\pi\right]-\frac{2k_{12}W^2}{\pi aE'}\ln\left(\cos\frac{\pi a}{W}\right)\right\}^{-1} \tag{38}$$

$E'=E$ for plane-stress, and $E'=E/(1-\nu^2)$ for plane-strain deformation. Expressions (35)–(38) reduce to Eqs. (24)–(27) in a natural way when $k_{22}=k_{12}=0$. Thus, we shall use expressions (35)–(38) for both unbridged and bridged cases, with the constant pseudo-tractions on the crack faces given by (33)–(34).

We obtained above the pseudo-tractions on the crack faces from the asymptotic analysis. They are found to be constants (in an average sense only for bridged cracks) and dependent upon the geometry of the crack arrays. Wang et al. (1999) presented the solution for the doubly periodic rectangular array

of cracks under unidirectional tension, i.e. the result in Eqs. (24) and (35). They compared the overall Young modulus calculated using this pseudo-traction and that obtained from an accurate numerical solution of the integral equation. It was found that the asymptotic solution gave results of good accuracy for unbridged cracks at low to moderate levels of conventional crack density ($a^2/(WH) = 0$–0.25) and relative crack length (2a/W = 0–0.4). The accuracy for bridged cracks was even better. Thus, confidence can be placed on the above asymptotic solutions for low to moderate levels of conventional crack density and relative crack length.

In the formalism of the pseudo-traction technique, the COD/CSD, as will be seen below, is determined by the pseudo-traction only. An examination of Eq. (6) in Section 2.1 and Eqs. (33) and (34) shows that

$$T^{\mathrm{r}}_{2222} = \zeta^{\mathrm{r}}, \quad T^{\mathrm{d}}_{2222} = \zeta^{\mathrm{d}}; \qquad T^{\mathrm{r}}_{1212} = \frac{1}{2}\eta^{\mathrm{r}}, \quad T^{\mathrm{d}}_{1212} = \frac{1}{2}\eta^{\mathrm{d}} \tag{39}$$

where, again, the superscripts r and d refer to the rectangular and diamond-shaped array, respectively. Other components of T_{ijkl} are trivial and are neglected.

It is seen from Eq. (7) that the average COD/CSD is directly proportional to T_{ijkl}, as is the increment ΔC_{ijkl} in Eq. (10). Thus, for a given crack density, the effect of the crack interactions on the overall moduli of the cracked body will be dependent on the values of T_{ijkl}. For the two crack configurations of Fig. 4, it is seen that the values of $T^{\mathrm{r}}_{2222} = \zeta^{\mathrm{r}}$ and $T^{\mathrm{d}}_{2222} = \zeta^{\mathrm{d}}$ are different. It was argued in the beginning of this section that under unidirectional tension, the rectangular array will have the strongest shielding effect and diamond-shaped will have the strongest magnification effect. This argument is fully supported by the results of the above asymptotic analysis. For unbridged cracks, the value of $T^{\mathrm{r}}_{2222} = \zeta^{\mathrm{r}}$ is always less than 1. The second term in the curly brackets in Eq. (35), which is always positive, will therefore always result in a reduction of the pseudo-traction, and thus a reduction of the average COD. In contrast to T^{r}_{2222}, $T^{\mathrm{d}}_{2222} = \zeta^{\mathrm{d}}$ is always greater than 1 due to the crack interactions, so that the COD will increase. The magnification effect may become very significant for small values of H/W and large values of a/W. It is tempting to examine the case when $T^{\mathrm{d}}_{2222} = \zeta^{\mathrm{d}}$ tends to infinity, as $1 - 4\sin^2(\pi a/W)\mathrm{e}^{-2(H/W)\pi}[1 + 2(H/W)\pi]$ vanishes. In this case, if we assume that $\sin^2(\pi a/W) = 1$, i.e. $a/W = 1/2$, then $1 - 4\sin^2(\pi a/W)\mathrm{e}^{-2(H/W)\pi}[1 + 2(H/W)\pi] = 0$ would give $H/W = 0.428$. Accordingly, the conventional crack density parameter $a^2/(WH)$ would work out to be 0.58. This level of crack density is probably beyond the range of applicability of the current asymptotic analysis, and also probably beyond the range of applicability of any existing analytical method. Kachanov (1992) remarked that for the two-dimensional case, the densities in the range 0.25–0.35 could be regarded as very high. On the other hand, under in-plane shear loading, as was to be expected, the value of $2T^{\mathrm{r}}_{1212} = \eta^{\mathrm{r}}$ is greater than 1, and that of $2T^{\mathrm{d}}_{1212} = \eta^{\mathrm{d}}$ is less than 1. These results are valid, provided $H/W > 1/(2\pi)$. A configuration where $H/W < 1/(2\pi)$, which is probably beyond the range of applicability of the asymptotic analysis, is unlikely to occur in reality. Thus, the argument that under in-plane shear loading, the rectangular array has strongest magnification crack interaction and the diamond-shaped array has the strongest shielding crack interaction is confirmed by the asymptotic analysis. For all the loading conditions and crack arrays, the crack bridging simply reduces the pseudo-tractions and thus prevents the degradation of the overall moduli of the cracked body.

4. Overall moduli and bounds

After calculating T_{2222} and T_{1212} from Eq. (39), we can calculate the values of ΔC_{2222} and ΔC_{1212} using Eq. (10). For this, we also need B_{ij} which relates the pseudo-traction to the average COD/CSD

$[\bar{u}_i]$. For an isotropic material, B_{ij} is proportional to a unit tensor. The off-diagonal components representing normal-shear coupling are zero (Kachanov, 1992). For the cases in the present paper, we need B_{11} and B_{22} for an array of periodic collinear cracks subjected to uniform pseudo-tractions given by Eqs. (33) and (34), respectively. These can be found in the work by Deng and Nemat-Nasser (1992), namely,

$$B_{11} = B_{22} = -\frac{2W^2}{\pi a E'} \ln\left(\cos\frac{\pi a}{W}\right) \tag{40}$$

which reduce to $B_{11} = B_{22} = \pi a E'$ for a single crack in an infinite body (Kachanov, 1992) when a/W approaches zero.

Substituting Eqs. (39) and (40) into Eq. (9), and after some manipulations, we get

$$\frac{E'}{E'_{22}} = 1 - \frac{4W}{\pi H} \ln\left(\cos\frac{\pi a}{W}\right) \begin{Bmatrix} \zeta^{\mathrm{r}} \\ \zeta^{\mathrm{d}} \end{Bmatrix} \tag{41}$$

$$\frac{\mu}{\mu_{12}} = 1 - \frac{2W}{\pi H(1+\nu)} \ln\left(\cos\frac{\pi a}{W}\right) \begin{Bmatrix} \eta^{\mathrm{r}} \\ \eta^{\mathrm{d}} \end{Bmatrix} \tag{42}$$

where μ_{12} is the overall shear modulus of the cracked body in the xy-plane (Fig. 4). ν is the Poisson ratio of the uncracked isotropic body. If the cracked body in Fig. 4 is in a plane-stress state of deformation, E'_{22} is simply the Young modulus of the material in the direction perpendicular to the crack faces, whence $E' = E$ for an isotropic medium. In this paper, for the purpose of seeking the overall Young modulus E_{22}, we simply consider the plane-stress state of deformation. Therefore, we get the following upper and lower bounds on the normalised overall Young and in-plane shear moduli:

$$\left(\frac{E_{22}}{E}\right)^{\mathrm{U}} = \left[1 - \zeta^{\mathrm{r}} \frac{4W}{\pi H} \ln\left(\cos\frac{\pi a}{W}\right)\right]^{-1} \tag{43}$$

$$\left(\frac{E_{22}}{E}\right)^{\mathrm{L}} = \left[1 - \zeta^{\mathrm{d}} \frac{4W}{\pi H} \ln\left(\cos\frac{\pi a}{W}\right)\right]^{-1} \tag{44}$$

$$\left(\frac{\mu_{12}}{\mu}\right)^{\mathrm{U}} = \left[1 - \eta^{\mathrm{d}} \frac{2W}{\pi H(1+\nu)} \ln\left(\cos\frac{\pi a}{W}\right)\right]^{-1} \tag{45}$$

$$\left(\frac{\mu_{12}}{\mu}\right)^{\mathrm{L}} = \left[1 - \eta^{\mathrm{r}} \frac{2W}{\pi H(1+\nu)} \ln\left(\cos\frac{\pi a}{W}\right)\right]^{-1} \tag{46}$$

where the superscripts U and L refer to the upper and lower bounds, respectively.

For bridged cracks, we introduce two non-dimensional parameters

$$\mathscr{A} = \frac{2k_{22}a}{\pi E}, \qquad \mathscr{B} = \frac{2k_{12}a}{\pi E} \tag{47}$$

where the former was introduced by Wang et al. (1999). Thus, the parameters in Eqs. (35)–(38) are rewritten as

$$\zeta^{\mathrm{r}} = \left\{1 + 4\sin^2\frac{\pi a}{W}\mathrm{e}^{-2(H/W)\pi}\left[1 + 2\frac{H}{W}\pi\right] - \mathscr{A}\left(\frac{a}{W}\right)^2\ln\left(\cos\frac{\pi a}{W}\right)\right\}^{-1} \tag{48}$$

$$\zeta^{\mathrm{d}} = \left\{1 - 4\sin^2\frac{\pi a}{W}\mathrm{e}^{-2(H/W)\pi}\left[1 + 2\frac{H}{W}\pi\right] - \mathscr{A}\left(\frac{a}{W}\right)^2\ln\left(\cos\frac{\pi a}{W}\right)\right\}^{-1} \tag{49}$$

$$\eta^{\mathrm{r}} = \left\{1 + 4\sin^2\frac{\pi a}{W}\mathrm{e}^{-2(H/W)\pi}\left[1 - 2\frac{H}{W}\pi\right] - \mathscr{B}\left(\frac{a}{W}\right)^2\ln\left(\cos\frac{\pi a}{W}\right)\right\}^{-1} \tag{50}$$

$$\eta^{\mathrm{d}} = \left\{1 - 4\sin^2\frac{\pi a}{W}\mathrm{e}^{-2(H/W)\pi}\left[1 - 2\frac{H}{W}\pi\right] - \mathscr{B}\left(\frac{a}{W}\right)^2\ln\left(\cos\frac{\pi a}{W}\right)\right\}^{-1} \tag{51}$$

The values of $\mathscr{A}$ and $\mathscr{B}$ depend on the material, that is, the matrix for a fibre-reinforced composite material, and on the bridging mechanism. Their magnitudes can be quite different, say, for short fibre-reinforced cementitious composite materials (Karihaloo et al., 1996) and short fibre-reinforced ceramic composite materials (Nemat-Nasser and Hori, 1987). In the following, we consider two cases with $\mathscr{A} = \mathscr{B} = 0.05$ and 0.50, respectively.

5. Results and discussion

In Fig. 5(a) and (b), the asymptotic bounds for unbridged cracks are compared with the overall moduli predicted by the dilute distribution solution (Deng and Nemat-Nasser, 1992), the differential scheme and the self-consistent method for $H/W = 0.5$ and 1.0, respectively. For the last two methods, the procedures described in the above paper are used. For large values of H/W, a large value of $a^2/(WH)$ will correspond to a very large a/W. For example, the configuration where $H/W = 1.0$ and $a^2/(WH) = 0.20$ corresponds to $a/W = 0.445$, which means the neighbouring tips of two collinear cracks are nearly touching each other. In all calculations, $\nu = 0.3$ is used in Eqs. (45) and (46).

Fig. 5(a) and (b) reveal several features of the overall moduli. Firstly, the bounds on the normalised overall in-plane shear modulus μ_{12}/μ are much closer than those on the overall normalised Young modulus E_{22}/E for the shown values of H/W and the crack density. Secondly, as expected and also widely reported in the literature, the differential scheme and the self-consistent method tend to give considerably low values of the overall moduli of cracked bodies, especially for large crack densities. Thus, for the rectangular and diamond-shaped arrays of cracks, the current results give a quantitative assessment of these two methods with regard to their accuracy. In Fig. 5(a) where $H/W = 0.5$, the results from the differential scheme appear to correspond to the lower bounds on E_{22}/E and μ_{12}/μ. In Fig. 5(b) where $H/W = 1.0$, which means weaker crack interactions, the differential scheme produces values of the overall moduli that are much smaller than even the lower bounds. On the other hand, the self-consistent method always predicts very low values of the overall moduli.

The dilute distribution solutions shown in Fig. 5(a) and (b) are obtained by neglecting the interactions among the crack rows, that is, by setting $\zeta^{\mathrm{r}} = \zeta^{\mathrm{d}} = \eta^{\mathrm{r}} = \eta^{\mathrm{d}} = 1$. Kachanov (1992) conducted a computational experiment on randomly distributed discrete parallel cracks and found that the result is very close to the approximation of non-interacting cracks. The current analytical results suggest that the overall moduli calculated for a row of collinear interacting cracks could be a good approximation to the

actual values for randomly distributed parallel cracks for they lie in the middle of the area enclosed by the upper and lower bounds. In Fig. 5(b), the bounds and the dilute distribution solution almost merge, indicating that when the vertical spacings between the cracks are in the order of the horizontal distances, the effect of crack stacks can be neglected. In this case, the overall moduli can be accurately predicted using a row of collinear cracks. It should, however, be noted that in the dilute distribution solution, the collinear interactions among the cracks are still considered. In that respect, it differs from the non-interacting approximation of Kachanov (1992).

Fig. 6(a) and (b) show the bounds for bridged cracks with different non-dimensional bridging stiffnesses, namely, $\mathscr{A} = \mathscr{B} = 0.05$ and $\mathscr{A} = \mathscr{B} = 0.50$, respectively. Again, the dilute distribution solution shown in these figures is obtained by neglecting the interactions among the cracks rows. However, the bridging effect is included in this case. For $\mathscr{A} = \mathscr{B} = 0.05$, that is, for weak bridging, the bounds on the overall moduli exhibit the same trend as those for the unbridged cracks, although it is noted that the bounds for the same crack configuration are closer than those for the unbridged cracks.

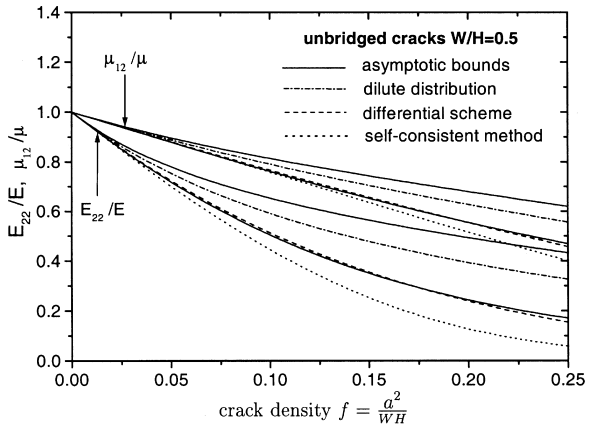

(a)

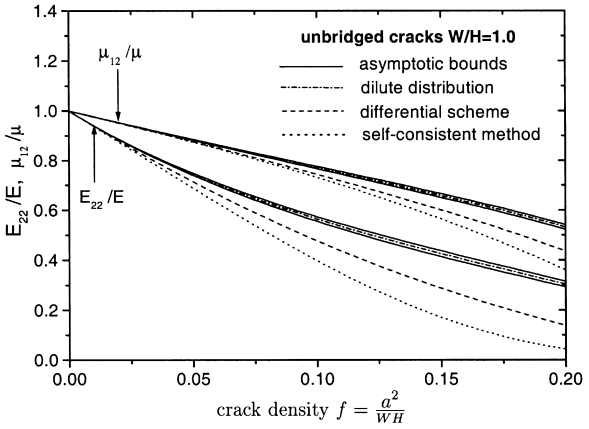

(b)

Fig. 5. Comparison of the asymptotic bounds with results predicted by the dilute distribution solution, the differential scheme and the self-consistent method for unbridged cracks.

For $\mathscr{A} = \mathscr{B} = 0.50$, that is, for strong bridging, the bounds are much closer than those for the unbridged cracks. Even for $H/W = 0.25$, the upper and lower bounds on the normalised shear moduli almost merge. This shows that when the cracks are bridged, the crack interactions become less important than those for the unbridged cracks. Under a strong bridging force, the crack opening/sliding is greatly reduced by the bridging tractions. This can be seen from the expressions (48)–(51). For unbridged cracks, the variation of the overall moduli is controlled by the second terms in the curly brackets in Eqs. (48)–(51), which represent the effect of the crack interactions. For bridged cracks, the effect of the third term comes into play. When this term dominates, the difference between the bounds diminishes.

For fibre-reinforced composite materials, it is known that the so-called strain hardening stage is characterised by multiple parallel microcracks under unidirectional tension. In this case, the randomness in the vertical spacing between the cracks may be greatly reduced compared with the case for monolithic materials. This is due to the load-transferring mechanism of the fibres. Such a phenomenon, for

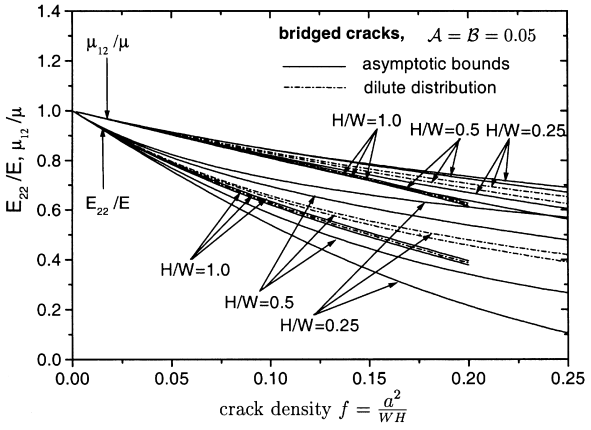

(a)

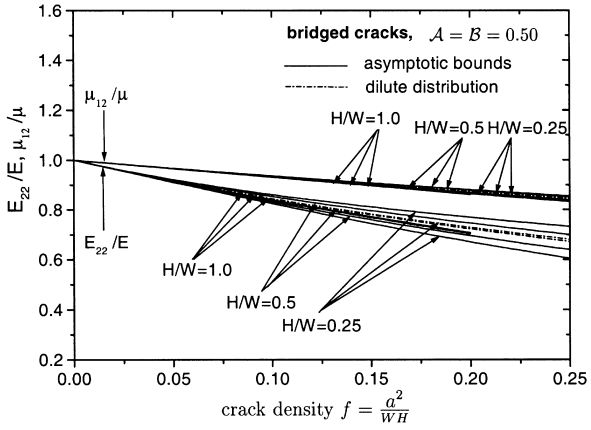

(b)

Fig. 6. Asymptotic bounds on overall moduli for bridged cracks. Also shown are the results when the interactions among the crack rows are neglected.

example, is depicted by the well-known ACK model (Aveston et al., 1971). For unbridged and bridged cracks, the stresses in the area adjacent to the crack faces excluding the area around the crack tips are much less than the applied stress. The stresses increase with the distance away from a crack. Thus, the cracks tend to form a somewhat regular pattern instead of a completely random one. It is also noted (Kachanov, 1992) that in real bodies, multiple crack configurations with both shielding and magnification interactions are possible. The results presented in this paper can be used to estimate the ranges of variation of the overall moduli of bodies containing naturally distributed parallel microcracks, which do not form regular arrays. In such cases, the geometrical parameters a, W and H have to be interpreted in a statistical sense.

Acknowledgements

The support of Yunnan Province of the People's Republic of China through the Collaborative Project No. B9807G is gratefully acknowledged by J. Wang and J. Fang.

References

Aveston, J., Cooper, G.A., Kelly, A., 1971. Single and multiple fracture. In: The Properties of Fibre Composites, Conference Proceedings of National Physical Laboratory. IPC, London, pp. 15–26.

Deng, H., Nemat-Nasser, S., 1992. Microcrack array in isotropic solids. Mech. Mater 13, 15–36.

Horii, H., Nemat-Nasser, S., 1985. Elastic fields of interacting inhomogeneities. International Journal of Solids and Structures 21, 731–745.

Hu, K.X., Chandra, A., Huang, Y., 1994. On interacting bridged-crack systems. International Journal of Solids and Structures 31, 599–611.

Ju, J.W., Chen, T.-M., 1994. Effective elastic moduli of two-dimensional brittle solids with interacting cracks. Part I: Basic formulations. J. Appl. Mech 61, 349–357.

Kachanov, M., 1987. Elastic solids with many cracks: a simple method of analysis. International Journal of Solids and Structures 23, 23–43.

Kachanov, M., 1992. Effective elastic properties of cracked solids: critical review of some basic concepts. Appl. Mech. Rev 45, 304–335.

Karihaloo, B.L., 1978. Fracture characteristics of solids containing doubly-periodic arrays of cracks. Proc. R. Soc. Lond A360, 373–387.

Karihaloo, B.L., Wang, J., Grzybowski, M., 1996. Doubly periodic arrays of bridged cracks and short fibre-reinforced cementitious composites. J. Mech. Phys. Solids 44, 1565–1586.

Karihaloo, B.L., Wang, J., 1997. On the solution of doubly periodic array of cracks. Mech. Mater 26, 209–212.

Nemat-Nasser, S., Hori, M., 1987. Toughening by partial or full bridging of cracks in ceramics and fibre reinforced composites. Mech. Mater 6, 245–269.

Tada, H., Paris, P.C., Irwin, G.R., 1973. The Stress Analysis of Cracks Handbook. Del Research Corporation, St Louis.

Wang, J., Fang, J. and Karihaloo, B.L., 1999. Asymptotics of multiple crack interactions and prediction of effective modulus. International Journal of Solids and Structures, in press.

Wu, S., Chudnovsky, A., 1990. The effective elastic properties of a linear elastic solid with microcracks. Engineering Fracture Mechanics 37, 653–659.